Published OnlineFirst March 24, 2009; DOI: 10.1158/0008-5472.CAN-08-2484

Research Article

Angiotensinogen Delays Angiogenesis and Tumor Growth of Hepatocarcinoma in Transgenic Mice

François Vincent,[1,4] Philippe Bonnin,[2] Maud Clemessy,[1] Jean-Olivier Contrerès,[2,3] Noël Lamandé,[1] Jean-Marie Gasc,[1] José Vilar,[2] Patricia Hainaud,[2,3] Gérard Tobelem,[2,3] Pierre Corvol,[1] and Evelyne Dupuy[2,3]

[1]Chaire de Médecine Expérimentale, INSERM U833, Collège de France; [2]Cardiovascular Research Center, INSERM U689 and [3]Institut des Vaisseaux et du Sang, Hôpital Lariboisière, Paris 7-Denis Diderot, Paris, France and [4]Service d'Explorations Fonctionnelles Physiologiques, Centre Hospitalier Universitaire Dupuytren, Limoges, France

Abstract

Angiotensinogen, a member of the serpin family, is involved in the suppression of tumor growth and metastasis. To investigate whether human angiotensinogen protects against tumor progression *in vivo*, we established an original bitransgenic model in which transgenic mice expressing human angiotensinogen (Hu-AGT-TG mice) were crossed with a transgenic mouse model of hepatocellular carcinoma (HCC-TG mice). Bitransgenic mice overexpressing human angiotensinogen (HCC/Hu-AGT-TG) had a significantly longer survival time than the HCC-TG mice and a reduction of both tumor growth and blood flow velocities in the liver. This antitumor effect of angiotensinogen is related to a reduced angiogenesis, impaired expression of endothelial arterial markers (active Notch4, Delta-like 4 ligand, and ephrin B2) with a decrease of arterial vessel density in HCC/Hu-AGT-TG mice liver. Overexpression of human angiotensinogen decreases angiogenesis, and prevents tumor sinusoids from remodeling and arterialization, thus delaying tumor progression *in vivo*. [Cancer Res 2009;69(7):2853–60]

Introduction

The role of angiogenesis to promote tumor progression and metastasis has been largely established. Numerous molecules have been reported to be involved in this process and blocking angiogenesis has given promising results in cancer therapies (1, 2). Tumor angiogenesis is also characterized by an abnormal vessel remodeling, and normalization of tumor vasculature represents an important therapeutic challenge (3). Angiotensinogen (AGT), the renin substrate, displays antiangiogenic properties *in vitro* and *in ovo*. AGT inhibits the proliferation of cultured endothelial cells, blocks the formation of capillary-like structures on Matrigel, and impairs neoangiogenesis in the chick chorioallantoic membrane assay (4, 5). AGT, mainly synthesized in the liver, is the only known precursor of angiotensin I (AngI; ref. 6). It can be considered as a combination of a short domain (AngI) located at the NH_2 terminus and a large one [des(AngI)AGT] which accounts for >97% of the molecule and has no known function (7). Homologies in terms of gene organization and protein structure suggest that AGT belongs to the serine proteinase inhibitor (serpin) family (8). Several serpins display antiangiogenic properties (9–12). More recently, we have shown that AGT impairs angiogenesis without altering the expression level of vascular growth factors through the induction of apoptosis and decreased endothelial cell proliferation (5). Furthermore, we showed that an adenovirus encoding human angiotensinogen (Hu-AGT) is able to inhibit tumor progression through an antiangiogenic effect in different mice models and represents a promising new strategy to block primary tumor growth and to prevent metastasis (13).

These results prompted us to investigate whether Hu-AGT exerts *in vivo* effects in a transgenic mouse model of cancer in terms of angiogenesis and tumor growth. For this purpose, we studied the effect of Hu-AGT in an original bitransgenic mouse model (HCC/Hu-AGT-TG mice), by crossing single transgenic mice developing hepatocarcinoma (HCC-TG mice) with single transgenic mice carrying the human AGT gene (Hu-AGT-TG mice). Hu-AGT-TG mice overproduced Hu-AGT with plasma levels 100-fold that of human plasma AGT levels. Hu-AGT is not cleaved by mouse renin. Angiotensin II (AngII) plasma concentration and blood pressure of Hu-AGT-TG mice had been previously reported and were indistinguishable from those of the control mice (14). HCC-TG mice developed hepatocarcinoma in multistep processes of tumor growth and tumor angiogenesis characterized by a strong remodeling of tumor sinusoids and the acquisition of an arterial phenotype by tumor sinusoidal endothelial cells (15, 16). We have shown that endothelial arterial markers such as Delta-like 4 ligand (Dll4), active Notch4, and ephrin B2 (17–20) are gradually upregulated during hepatocarcinoma progression (21). In this model, we have also developed noninvasive measurements of liver volume and neovascularization by conventional two-dimensional color-coded pulsed Doppler ultrasound imaging, allowing us to follow the efficacy of potential antiangiogenic factors (22). Because AGT is mainly synthesized in the liver, our bitransgenic mouse model is appropriated to study the potential antiangiogenic effect of AGT.

We show a significantly longer survival rate in HCC/Hu-AGT-TG compared with HCC-TG mice, with reduced tumor liver volume and angiogenesis associated with impaired blood flow velocities in tumor-feeding hepatic artery. In addition, Hu-AGT prevents the tumor sinusoids from their remodeling and arterialization.

Materials and Methods

Animal models. All of the animal procedures for the care and use of laboratory animals were conducted according to the guidelines of our

Note: Supplementary data for this article are available at Cancer Research Online (http://cancerres.aacrjournals.org/).

P. Bonnin, M. Clemessy, J-O. Contrerès, and N. Lamandé contributed equally to this work.

This work is dedicated to the memory of Jean Plouët, a great scientist who will remain dear to all his colleagues and friends.

Requests for reprints: François Vincent, Collège de France, Laboratoire de Médecine Expérimentale, INSERM U833-11 place Marcelin Berthelot, 75005 Paris, France. Phone: 33-14427-1653; Fax: 33-14427-1691; E-mail: francois.vincent@college-de-france.fr.

doi:10.1158/0008-5472.CAN-08-2484

Published OnlineFirst March 24, 2009; DOI: 10.1158/0008-5472.CAN-08-2484

institution and the Federation of European Laboratory Animal Science Association.

Transgenic mice expressing human angiotensinogen (Hu-AGT-TG mice). Hu-AGT-TG mice were kindly provided by Curt D. Sigmund (14). Briefly, the transgene, consisting of the human AGT gene plus ~1.2 kb upstream and 1.4 kb downstream, was injected into (C57/BL6/J × SJL/J)F_2 one-cell fertilized mouse embryos, thus generating transgenic mice. Because Hu-AGT is not cleaved by mouse renin, angiotensin II (AngII) plasma concentration and blood pressure of Hu-AGT-TG mice were indistinguishable from those of the control mice (14).

Transgenic mouse model of hepatocellular carcinoma (HCC-TG mice). The production of transgenic ASV-B mice, which develop hepatocellular carcinoma, has been previously described (15). The transgene was integrated on the Y chromosome, so the development of hepatocarcinoma was restricted to male mice, which were backcrossed with C57/BL6 mice at least 10-fold. Three major stages of the temporospatial progression of the HCC-TG mice and angiogenic processes have been previously described: hyperplastic (4–8 weeks), nodular (12 weeks), and diffuse carcinoma (16–24 weeks; ref. 16).

Generation of bitransgenic mice (HCC/Hu-AGT-TG). The bitransgenic mouse model (HCC/Hu-AGT-TG mice) was produced by crossing HCC-TG male with Hu-AGT-TG female mice. In these compound HCC/Hu-AGT-TG mice, the incidence of hepatocarcinoma was 100% and the production of Hu-AGT was 100-fold that in human plasma.

Survival. The outcome measure was estimated by overall survival duration in HCC-TG (n = 12) and HCC/Hu-AGT-TG (n = 12) mice groups. Survival duration was defined as the time from birth to death. The probability of surviving was estimated using the Kaplan-Meier product-limit method. Overall survival was calculated from the date of random assignment to the date of death. All statistical analyses in this study were carried out using the StatView 5.0 program (SAS Institute, Inc.).

Ultrasound study. Mice were subjected to ultrasound measurements using an echocardiograph (Vivid 7, GE Medical Systems Ultrasound) equipped with a 12-MHz linear transducer. Ultrasound study of the liver and time-averaged mean blood flow velocities measured in the hepatic and mesenteric arteries were performed in these mice as previously described (22). All ultrasound measurements were performed in the three transgenic mouse groups (HCC-TG (n = 12), HCC/Hu-AGT-TG (n = 12), Hu-AGT-TG (n = 8) mice) at different ages (4–24 weeks) corresponding to the main stages of hepatocarcinoma. Wild-type C57/BL6 mice were used as controls (n = 8). We previously showed that the liver volume, assessed by ultrasound, increased with the progression of hepatocarcinoma (22). Thus, we estimate that the liver volume reflected tumor growth.

Microangiography. Microangiographies were performed in two Hu-AGT, two HCC-TG, and two HCC/Hu-AGT-TG mice at 8, 12, and 16 weeks, respectively, as previously described (22) with modifications. Before the perfusion of the contrast agent, mesenteric artery and aorta upstream from the celiac trunk were ligated. Image acquisition with a digital X-ray transducer was performed and computerized. Quantification of arterial vessel density, within the liver, was calculated using specific software (Primed Microvision) and expressed as a percentage of pixels per image occupied by vessels in the total liver area.

Tissue preparation. Livers were obtained from HCC/Hu-AGT-TG (n = 4), HCC-TG (n = 4), Hu-AGT-TG (n = 2), and wild-type mice as controls (n = 2) at different ages corresponding to the main stages of hepatocarcinoma. Pieces of liver were frozen in liquid nitrogen for immunofluorescence or fixed in 4% paraformaldehyde in PBS and processed for paraffin histology (immunoperoxidase and *in situ* hybridization; ref. 23).

Immunohistochemistry and quantifications. CD31 (PECAM-1) was detected in liver sections by the antibody (rat purified anti-CD31, 1/100, clone MEC 13.3; BD Biosciences), after unmasking by proteolytic digestion (trypsin 250 μg/mL, 15 min at 37°C), secondary antibody (rabbit anti-rat, 1/400, BA4001; Vector Laboratories), tyramide signal amplification (indirect kit; Perkin-Elmer), and 3,3′-diaminobenzidine (DAB) was used as chromogen to reveal peroxidase activity. Laminin antigen was detected in liver sections by the antibody (rabbit anti-laminin, 1/100, L9393; Sigma), secondary antibody (goat anti-rabbit, 1/500, BA1000; Vector Laboratories), avidin-biotin-peroxidase complex (Vectastain ABC Elite kit; Vector Laboratories), and DAB was used as a chromogen for the peroxidase activity. Ki-67 antigen was detected in liver sections by the antibody (monoclonal rat anti-Ki-67, dilution 1/100, M7249; DakoCytomation), antigen retrieval with citrate buffer (pH 6), secondary antibody (goat anti-rat, dilution 1/500, BA4001; Vector Laboratories), avidin-biotin-peroxidase complex (Vectastain ABC Elite kit; Vector Laboratories), and DAB was used as a chromogen for the peroxidase activity. Quantification areas were performed in the nodules, at the nodular (12 weeks) and diffuse (16 weeks) stages. Three random nodules/section were scanned with a digital camera (DFC420, Leica). Quantifications of CD31 microvessel density or Ki-67–positive cells were calculated using specific software (IPLab, Ivision, Scanalytics) and were expressed as a percentage of pixels per surface unit of nodule.

Immunofluorescence stainings. Liver sections and immunofluorescence stainings were done as previously described (16, 21). The primary antibody was either omitted or the liver sections were incubated with a nonimmune IgG as negative control. Liver sections were incubated with recombinant mouse EphB4/Fc chimera, 1/20 (R&D Systems Europe), known to bind to ephrin B2, then with a goat anti-human IgG, Fcγ, 1/30 (Jackson ImmunoResearch Laboratory) followed by incubation with the Alexa Fluor 488 donkey anti-goat antibody (Interchim).

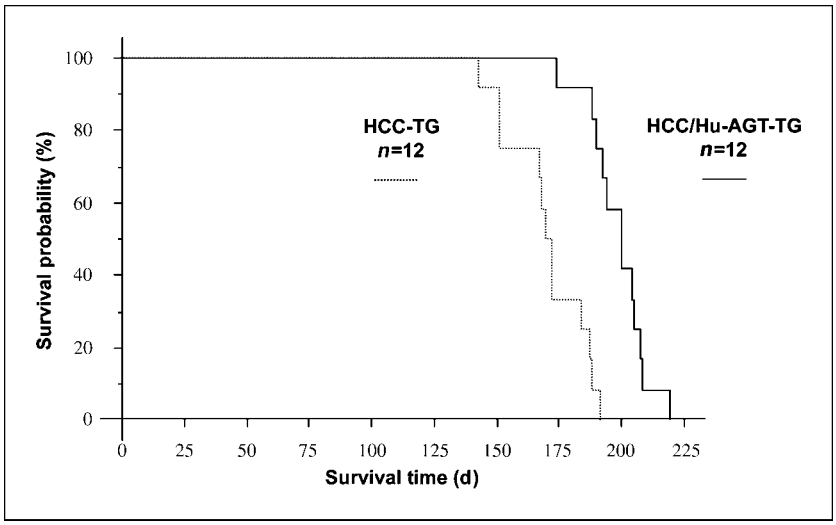

Figure 1. Kaplan-Meir analysis of survival in HCC-TG mice (*dotted line*) vs. bitransgenic mice (*full line*). $P < 0.0001$ (*n,* number of mice).

Published OnlineFirst March 24, 2009; DOI: 10.1158/0008-5472.CAN-08-2484

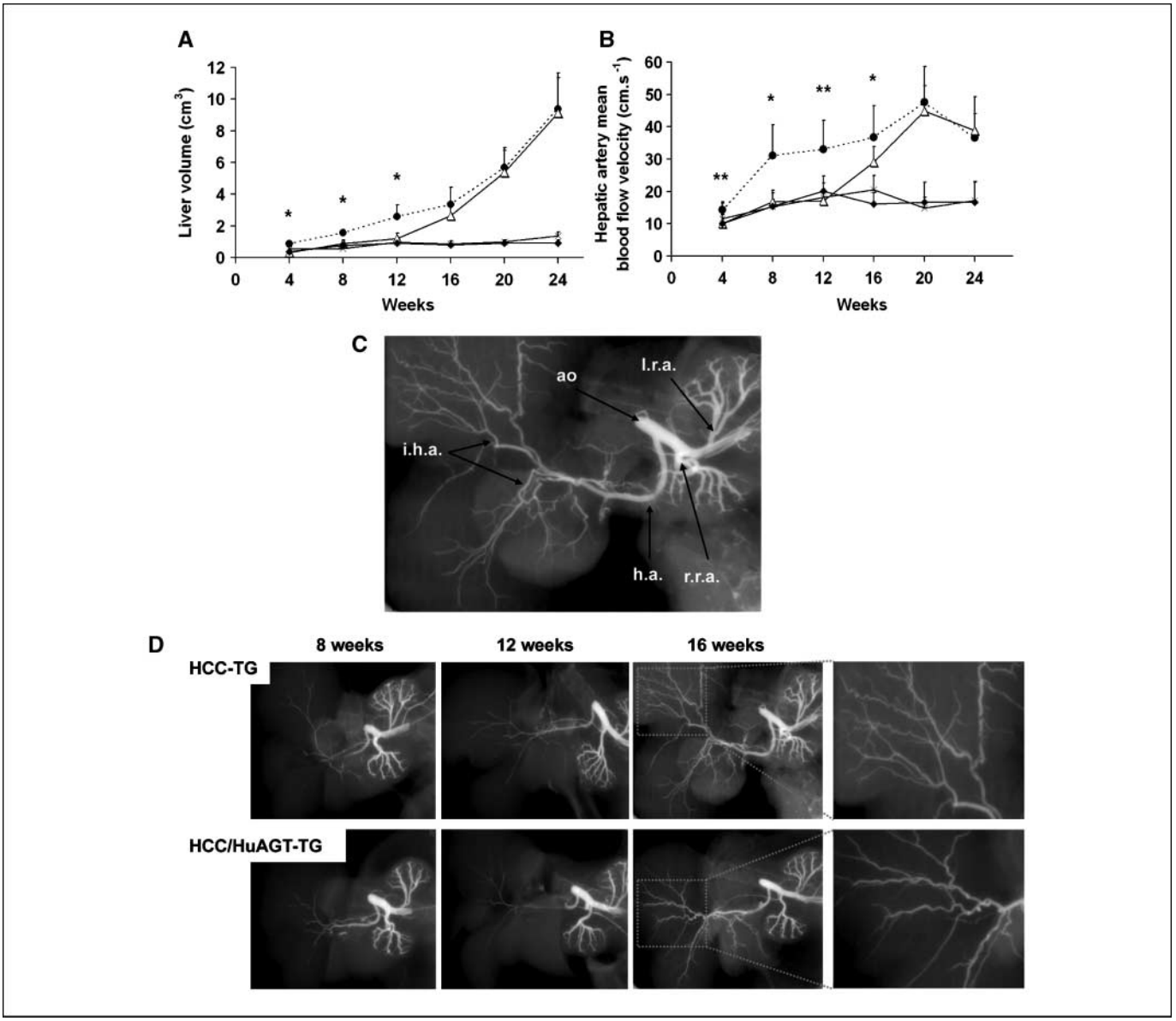

Figure 2. *A,* echo-derived volume of the liver in HCC-TG mice (●), bitransgenic mice (△), Hu-AGT-TG mice (♦), and control wild-type mice group (×). *Points,* mean of the liver volume for each group; *bars,* SD (*, $P < 0.001$, statistically significant for bitransgenic vs. HCC-TG mice). *B,* hepatic artery mean blood flow velocities in HCC-TG mice (●), HCC/Hu-AGT-TG mice (△), Hu-AGT-TG mice (♦), and control wild-type mice group (×). *Points,* mean for each group; *bars,* SD (*, $P < 0.05$; **, $P < 0.0001$, statistically significant for bitransgenic vs. HCC-TG mice). *C,* representative photomicrograph of computerized microangiography performed with a digital X-ray transducer in HCC-TG mouse at 16 wk (*ao,* aorta; *h.a.,* hepatic artery; *i.h.a.,* intrahepatic arteries; *l.r.a.,* left renal artery; *r.r.a.,* right renal artery). *D,* microangiographies in HCC-TG and HCC/Hu-AGT-TG mice at 8, 12, and 16 wk; *insets,* intrahepatic arteries at 16 wk.

***In situ* hybridization.** Single-strand sense and antisense riboprobes, labeled with ^{35}S-UTP (Amersham Biosciences), were generated by *in vitro* transcription from a 1,659-bp human AGT cDNA, cloned in pECEI. The *in situ* hybridization method has been described in detail (23).

Protein extraction and Western immunoblotting. The method has been previously described (21). Protein concentrations were determined using the BCA protein reagent assay kit (Pierce). The protein samples (75 μg) were resolved by 10% SDS-PAGE under reducing conditions and transferred onto nitrocellulose membranes using 25 mmol/L of Tris, 20 mmol/L of glycine, and 15% methanol. The membranes were blocked by incubation in TBS containing 5% nonfat milk powder for 90 min at room temperature. The membranes were incubated overnight at 4°C with specific antibodies against the active form of Notch4 (1/200, Upstate Euromedex), Dll4 (1/200, Santa Cruz Biotechnology), or ephrin B2 (1/200, Santa Cruz Biotechnology). The membrane was then incubated with horseradish peroxidase–conjugated anti-rabbit or anti-goat IgG (Jackson ImmunoResearch Laboratory). Antibody binding was revealed with the enhanced chemiluminescence system (Amersham Pharmacia Biotech).

Human AGT RIA. Blood was collected into chilled tubes containing heparin (Sarstedt). The plasma concentration of human AGT was measured indirectly, as described by Clauser and colleagues using recombinant human renin (24). Briefly, aliquots of mouse plasma samples were incubated for 1 h at 37°C. AngI concentrations produced were determined by RIA (25).

Statistics. All ultrasound measurements were compared by ANOVA and post hoc unpaired Student's *t* test. Results are expressed as mean ± SD. Mann-Whitney test was used for statistical analysis of CD31 and Ki-67 quantifications.

Published OnlineFirst March 24, 2009; DOI: 10.1158/0008-5472.CAN-08-2484

Results

Survival. Bitransgenic mice (HCC/Hu-AGT-TG) had a significantly longer survival time than the HCC-TG mice group. The median survival time was 200 days (range, 174–219) in the HCC/Hu-AGT-TG mice group and 170 days (range, 143–191) in the HCC-TG mice group ($P < 0.0001$; Fig. 1).

AGT reduces liver volume, blood flow velocities, and arterial vessel density in bitransgenic mice. Echo-derived volume of the liver increased significantly by 6.4-fold in hepatocarcinoma transgenic mice and increased (1.8-fold and 1.7-fold) in wild-type controls and in Hu-AGT-TG mice, respectively, from 4 to 24 weeks (Fig. 2*A*). In bitransgenic mice, liver volume was significantly decreased compared with HCC-TG mice: 3-fold (0.30 versus 0.90 cm^3) at 4 weeks, 1.8-fold (0.90 versus 1.60 cm^3) at 8 weeks, and 2.2-fold (1.20 versus 2.6 cm^3) at 12 weeks, respectively (Fig. 2*A*). From the 16th week, the difference in liver volume between bitransgenic and HCC-TG mice was abolished (Fig. 2*A*). These results suggested that until 12 weeks, the liver volume was significantly smaller (50%) in bitransgenic mice compared with HCC-TG mice.

Hepatic time-averaged mean blood flow velocity was significantly higher in HCC-TG mice than in Hu-AGT-TG and wild-type control mice groups from 4 to 24 weeks (Fig. 2*B*). Hepatic mean blood flow velocity was significantly lower in bitransgenic mice compared with HCC-TG mice by 30% (10 versus 14.4 cm/s) at 4 weeks, 46% (16.8 versus 31.1 cm/s) at 8 weeks, 48% (17.1 versus 33 cm/s) at 12 weeks, and 21% (29 versus 36.8 cm/s) at 16 weeks (Fig. 2*B*). From the 20th week, there was no significant difference in hepatic mean blood flow velocity between bitransgenic and HCC-TG mice groups (Fig. 2*B*). In all animal groups, no differences in blood flow velocities were observed in the mesenteric artery used as control.

The microangiography revealed the aorta (*ao*), the left (*l.r.a.*) and right renal (*r.r.a.*) arteries, the hepatic artery (*h.a.*) and intra hepatic artery (*i.h.a.*; Fig. 2*C*). The arterial phase revealed a reduced liver vascular network in the bitransgenic mice compared with HCC-TG mice at the hyperplastic (8 weeks), nodular (12 weeks), and diffuse (16 weeks) stages (Fig. 2*D*). The intrahepatic artery vessels seemed less branched (Fig. 2*D, right*). In addition, arterial vessel density within the liver was reduced by 6% at 8 weeks, 23% at 12 weeks, and 31% at 16 weeks in bitransgenic compared with HCC-TG mice.

AGT reduces tumor angiogenesis in bitransgenic mice. CD31 stained both sinusoids and large vessels derived from the portal tract. At the hyperplastic stage (8 weeks), CD31 staining did not show any detectable difference between bitransgenic, HCC-TG, and wild-type mice livers (Fig. 3*A*). In contrast, at the nodular (12 weeks) and the diffuse stages (16 weeks), CD31 immunostaining was markedly reduced in the bitransgenic compared with HCC-TG livers (Fig. 3*A*). At 12 and 16 weeks, the number of CD31-positive sinusoids within nodules was significantly reduced in bitransgenic compared with HCC-TG livers (Fig. 3*A*). The microvessel density count was 8.8 ± 0.7% versus 13.5 ± 4.2%, respectively ($P < 0.005$) at 12 weeks and 10.1 ± 1.8% versus 19.0 ± 4.5%, respectively ($P < 0.01$) at 16 weeks (Fig. 3*B*). At 20 weeks, this difference disappeared between bitransgenic and HCC-TG livers.

Expression of the active form of Notch4, Dll4, and ephrin B2 were reduced in bitransgenic mice. The active form of Notch4 was barely detected by Western blotting in wild-type and Hu-AGT livers regardless of mouse age (8–20 weeks), and it increased from the hyperplastic stage in HCC-TG livers (Fig. 4*A*). In bitransgenic livers, the expression of active Notch4 was markedly inhibited by 65% and 55% up to 12 weeks (Fig. 4*A*). At 16 weeks, at which time

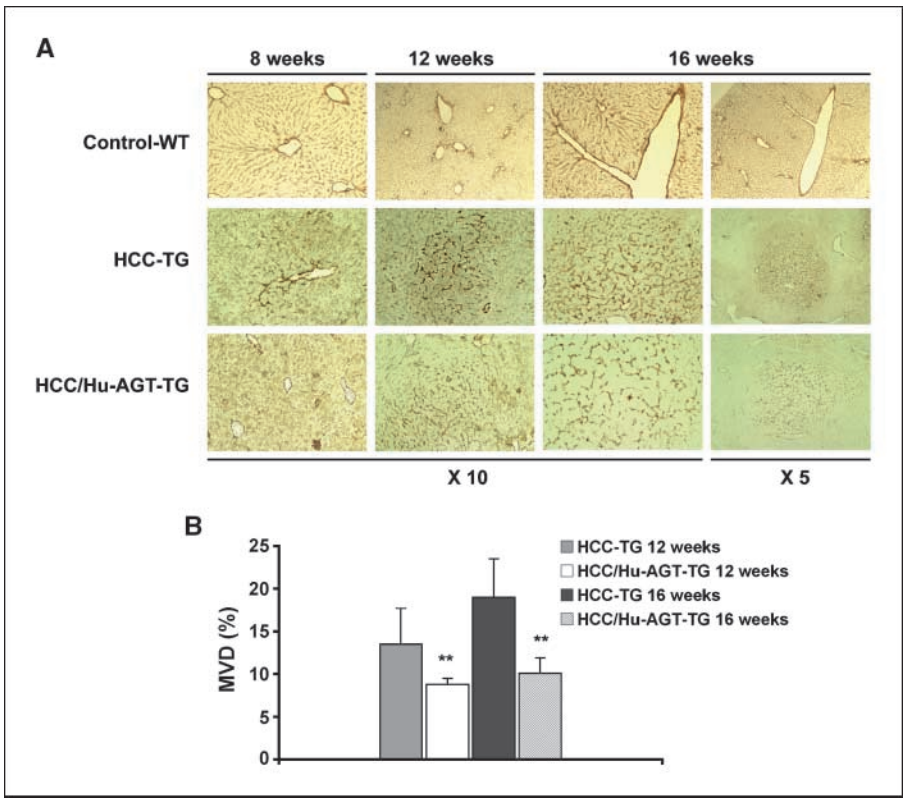

Figure 3. *A,* CD31 immunostaining at 8, 12, and 16 wk in HCC-TG, bitransgenic, and control/wild-type mice groups. At 8 wk, staining was not different between wild-type, bitransgenic, and HCC-TG mice. At 12 and 16 wk, CD31 staining of sinusoids was decreased in bitransgenic vs. HCC-TG livers. *B,* analysis of microvessel density (*MVD*) in nodules at 12 and 16 wk in HCC-TG and bitransgenic mice groups. At 12 and 16 wk, the number of CD31-positive sinusoids within nodules were significantly lower in bitransgenic vs. HCC-TG livers (**, $P < 0.01$).

Published OnlineFirst March 24, 2009; DOI: 10.1158/0008-5472.CAN-08-2484

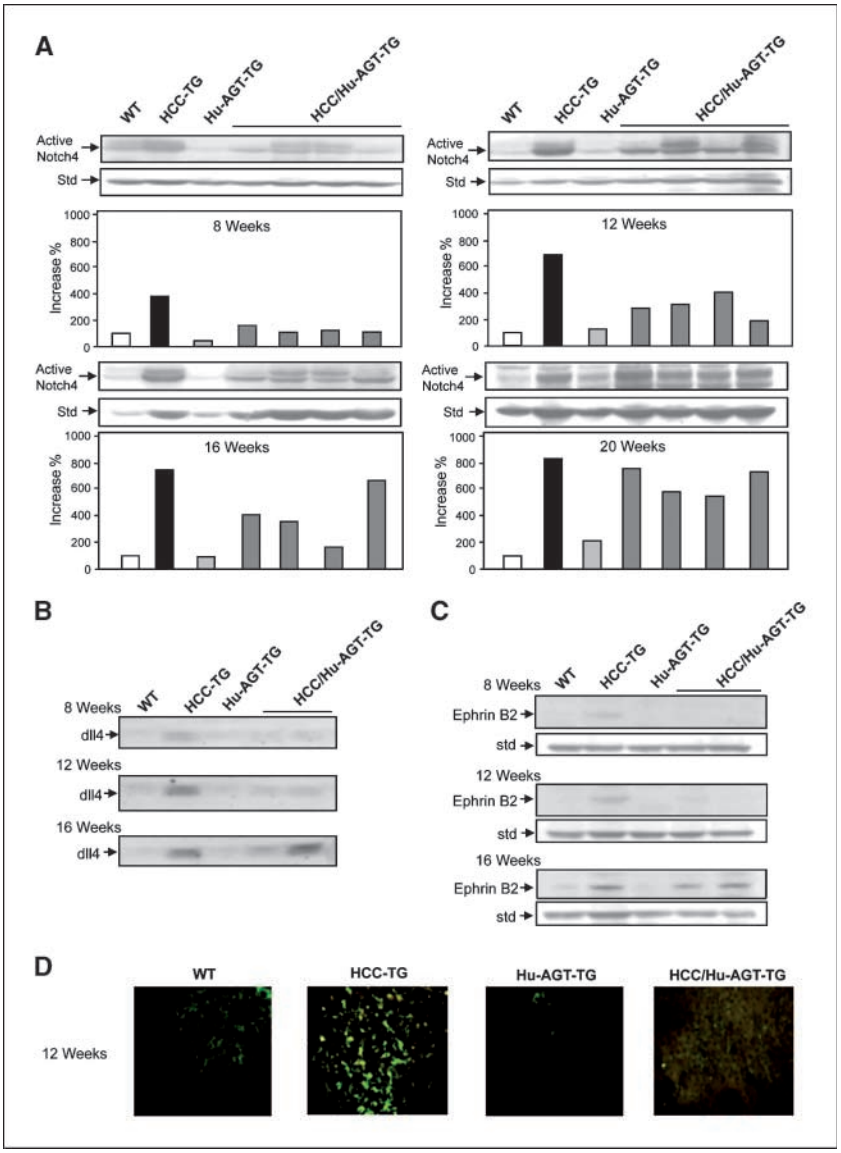

Figure 4. Expression of arterial markers in livers. *A,* detection of active Notch4 in Hu-AGT-TG and bitransgenic mice by Western blot. *Top gels,* bands corresponding to the truncated and active forms of Notch4 (60 kDa); *bottom gels,* bands corresponding to a nonspecific protein (*std*) revealed with the anti-Notch4 antibody which serve as an internal control of loading. Quantification: densitometric quantification of the bands corresponding to the active form of Notch4 and the internal control (*std*) were performed using Image Master 1D elite Amersham Pharmacia software. Results were expressed as the ratio of Notch4 to control band values for each condition and were normalized to that of normal mice (100%). *B,* bands corresponding to Dll4 (74 kDa). The equal loading of protein was assessed by imaging Ponceau S–stained nitrocellulose membrane after transfer using Amersham Pharmacia Image Master VDS-CL imager. *C,* bands corresponding to ephrin B2 (55 kDa; *top gels*). Bands corresponding to a nonspecific protein (*std*) revealed with the anti-ephrin B2 antibodies which serve as an internal control of loading (*bottom gels*). *D,* ephrin B2 immunostaining at 12 wk, ephrin B2 was not expressed in wild-type (*WT*), Hu-AGT, whereas ephrin B2–positive sinusoidal endothelial cells were detected in HCC-TG. In contrast, no ephrin B2 staining was observed in bitransgenic as for wild-type and Hu-AGT livers. Original magnification, ×40.

tumor growth and neovascularization began to escape to Hu-AGT, this inhibition was weaker (47%) and more heterogeneous in the HCC/Hu-AGT-TG group, and was close to the values obtained in HCC-TG livers at 20 weeks (Fig. 4*A*). We also investigated the expression of Dll4, one ligand of Notch4. Regardless of mouse age (8–16 weeks), Dll4 protein was not detected in wild-type and Hu-AGT mice, and we confirmed that its level greatly increased from the early stage in HCC-TG mice (Fig. 4*B*). In bitransgenic (HCC/Hu-AGT-TG) mice, Dll4 was not detectable at the hyperplastic stage (8 weeks), barely detected at the nodular stage (12 weeks), and an escape occurred at the diffuse stage (16 weeks; Fig. 4*B*). Because active Notch4 acts upstream of ephrin B2, we have also investigated the expression of ephrin B2. At 8 weeks, ephrin B2 was not detected in wild-type Hu-AGT mice, whereas an up-regulation of ephrin B2 was observed in HCC-TG mice (Fig. 4*C*). In contrast, in the HCC/Hu-AGT-TG mice, the ephrin B2 expression was ablated at 8 and 12 weeks (Fig. 4*C*) as confirmed by ephrin B2 immunostaining (Fig. 4*D*). In bitransgenic livers, the reduction of the sinusoid arterialization was confirmed by laminin staining (Supplementary Fig. S1).

AGT displayed an antiproliferative effect in tumor hepatocytes. To determine if AGT might also inhibit hepatocyte proliferation, we performed a Ki-67 staining. Few isolated Ki-67–positive hepatocytes were observed in wild-type (8–16 weeks; Fig. 5*A*) and in Hu-AGT-TG mice (data not shown). In HCC-TG, Ki-67–positive hepatocytes were depicted at 8 weeks (Fig. 5*A*). Their number greatly increased from the 12th week to the 16th week (Fig. 5*A*). Moreover, the most proliferative hepatocytes were observed within the nodule (Fig. 5*A*). In contrast, in bitransgenic mice, at 8 weeks, fewer Ki-67–positive hepatocytes were observed (Fig. 5*A*). Ki-67–positive hepatocytes began to be detected at 12 weeks but at a lesser extent than those observed in HCC-TG and increased at 16 weeks (Fig. 5*A*). The Ki-67–positive hepatocyte counts were 3.6 $\pm$ 1.8% versus 9.1 $\pm$ 2.4%, respectively, for bitransgenic and HCC-TG mice ($P < 0.01$) at 12 weeks, and 4.3 $\pm$ 2.1% versus 11.6 $\pm$ 2.7% ($P < 0.001$) at 16 weeks (Fig. 5*B*).

Expression of Hu-AGT in livers. In bitransgenic livers, *in situ* hybridization of human AGT mRNA showed a heterogeneous pattern expression of Hu-AGT at 12 and 16 weeks (Fig. 6*A* and *B*). We distinguished two regions of Hu-AGT mRNA expression:

Published OnlineFirst March 24, 2009; DOI: 10.1158/0008-5472.CAN-08-2484

a nodular region with low-level expression of Hu-AGT and an internodular region with a higher level of expression (Fig. 6*A*). At 12 weeks, the stage at which nodular structures appeared, a decreased expression of Hu-AGT mRNA was observed in nodule compared with the internodular regions (Fig. 6*A*). This discrepancy increased at 16 weeks, the stage at which the number and size of nodules increased, with a lower expression of Hu-AGT mRNA in nodules compared with the internodular regions (Fig. 6*A*). From 16 to 24 weeks (diffuse stage), differences in Hu-AGT mRNA expression persisted between nodular and internodular regions in bitransgenic livers (data not shown). From 8 to 16 weeks, expression of Hu-AGT mRNA was homogeneous in Hu-AGT mice without any detection of Hu-AGT mRNA in HCC-TG mice as expected (Fig. 6*B*). In bitransgenic livers, Hu-AGT mRNA expression was homogeneous in the internodular regions at 8 and 12 weeks (Fig. 6*B*). At 16 weeks, we confirmed, by *in situ* hybridization, the lower expression of Hu-AGT mRNA in nodules compared with the internodular regions (Fig. 6*B*).

Plasma concentrations of Hu-AGT. From 4 to 12 weeks, plasma concentration of Hu-AGT increased in bitransgenic mice group: 8,354 ± 4,469 nmol/L at 4 weeks, 12,208 ± 4,495 nmol/L at 8 weeks, and 13,041 ± 2,739 nmol/L at 12 weeks. From 16 to 20 weeks, the plasma concentration of Hu-AGT decreased in bitransgenic mice: 12,125 ± 1,956 nmol/L at 16 weeks and 5,781 ± 262 nmol/L at 20 weeks.

Discussion

An antiangiogenic and antitumor effect of AGT has been previously shown *in vitro* and in tumor xenograft models (4, 5, 13). In this study, we have hypothesized that AGT would antagonize the tumor angiogenesis and consequently delay tumor growth in the murine model of hepatocarcinoma. We used an original model of bitransgenic mice overexpressing human AGT and developing hepatocarcinoma to analyze the spatial and temporal effect of Hu-AGT in angiogenesis and tumor progression. Here, we show *in vivo* that Hu-AGT delays tumor growth and prolongs survival, reduces tumor angiogenesis, and prevents the tumor sinusoids from their abnormal remodeling and arterialization. Arterial blood flow velocities recorded upstream from an organ give information on the development of the downstream vessels, vascular resistance, and represent a functional assessment of vessels (26). Thus, hepatic blood velocities recorded in the hepatic artery was used to assess downstream vessels functionality, i.e., an increase in HCC-TG mice related to abnormal liver vessels (22). Here, hepatic artery blood flow velocities were lowered in bitransgenic mice from 4 to 16 weeks without any significant difference compared with wild-type mice until 12 weeks. Normally, the liver vasculature is mainly supplied by the portal vein (80%) and 20% by the hepatic artery. In HCC-TG mice, the arterial phase is markedly increased (22). Here, we observed a concomitant decrease in arterial inflow and arterial vessel density in bitransgenic mice until 16 weeks. Thus, Hu-AGT protects the hepatic vasculature from arterial remodeling. Moreover, in bitransgenic livers, CD31 staining shows more regular and less dilated sinusoids in favor of their phenotype normalization. Hepatocarcinoma is a hypervascular tumor characterized by a capillarization of the sinusoids, normally from venous origin (27). We have previously shown, in HCC-TG livers, a temporal and spatial up-regulation of endothelial arterial markers (Dll4, active Notch4, and ephrin B2) during abnormal remodeling of tumor sinusoids (21). In bitransgenic livers, the expression of

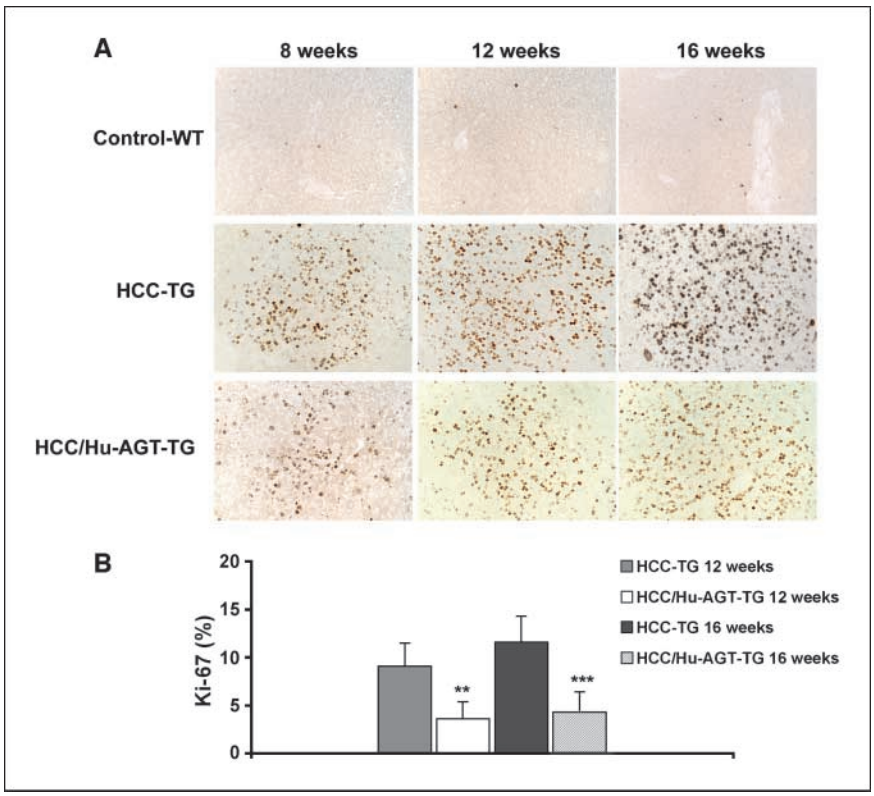

Figure 5. Ki-67 immunostaining. *A,* only few isolated Ki-67–positive hepatocytes were observed from 8 to 16 wk in wild-type livers. In HCC-TG livers, the number of Ki-67–positive hepatocytes greatly increased from the 8th wk. In bitransgenic livers, Ki-67 staining of hepatocytes was decreased compared with HCC-TG livers from 8 to 16 wk. Original magnification, ×10. *B,* at 12 and 16 wk, Ki-67–positive hepatocyte counts were significantly reduced in HCC/Hu-AGT-TG vs. HCC-TG livers (**, $P < 0.01$; ***, $P < 0.001$).

Published OnlineFirst March 24, 2009; DOI: 10.1158/0008-5472.CAN-08-2484

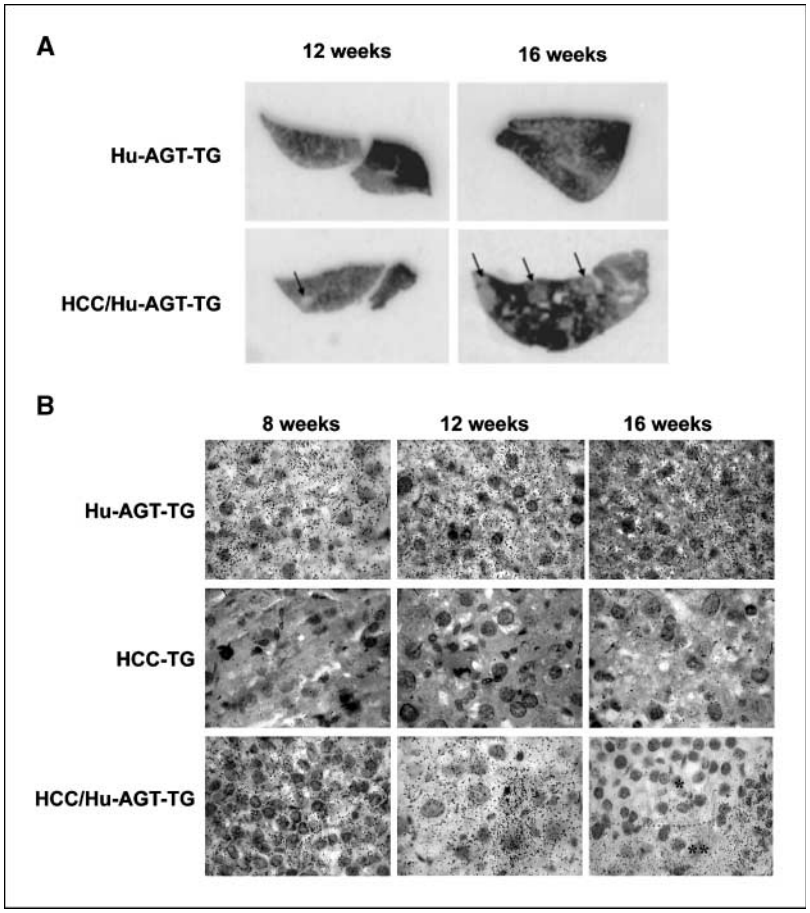

Figure 6. Expression of Hu-AGT mRNA in Hu-AGT-TG, HCC-TG and HCC/Hu-AGT-TG livers. *A,* scannings of Hu-AGT-TG and HCC/Hu-AGT-TG livers at 12 and 16 wk (X-ray films) after exposure of liver sections hybridized with a 35S-labeled probe to Hu-AGT. At 12 and 16 wk, *in situ* hybridization analysis showed a low expression of Hu-AGT mRNA levels in nodules (*arrows*), and in contrast, a high expression of Hu-AGT mRNA levels in internodular regions. *B, in situ* hybridization of human AGT mRNA in Hu-AGT-TG, HCC-TG, and HCC/Hu-AGT-TG livers (8–16 wk). At 16 wk, Hu-AGT mRNA expression was reduced in the nodular (*) compared with the internodular regions (**) in HCC/Hu-AGT-TG livers. Original magnification, ×40.

arterial markers was impaired. At the hyperplastic stage, in which the arterial vessel density was reduced by 6%, we noted a 65% inhibition in Notch4 levels, without any detection of Dll4 and ephrin B2. At the nodular stage (12 weeks), the arterial vessel density was reduced by 23% and the number of CD31 vessels, within nodules, by 65%, whereas Dll4 and ephrin B2 were only barely detectable. Thus, in HCC/Hu-AGT-TG livers, the decrease in arterial markers was higher than that of arterial vessel density at early stages of hepatocarcinoma. Therefore, the decrease in endothelial arterial markers was not simply related to the decrease in arterial vessel density. Dll4 was overexpressed in tumor vessels (20, 21, 28), but paradoxically, the inhibition of Dll4 signaling reduces tumor growth by promoting an excessive nonproductive angiogenesis (29, 30). In xenograft models, the tumor is avascular and the neovessel formation proceeds from the host mouse. In our transgenic model, the process is different because tumor angiogenesis proceeds from the native intrahepatic vasculature. In our bitransgenic model, reduction of Dll4 by Hu-AGT was not associated with an increase of nonfunctional vessels as assessed by ultrasound studies and microangiographies.

The Notch and ephrin families, largely involved in vascular development (17, 31), also participate in vessel remodeling in adult mice (18, 32). Thus, AGT in reducing Dll4, active Notch4, and its target gene, ephrin B2, would play a role in the maintenance of normal liver vessels until the 16th week.

Here, we showed that AGT mRNA expression was decreased in nodules compared with internodular regions. From the diffuse stage of hepatocarcinoma (16 weeks), T-SV40–positive hepatocyte ceased to express AGT. Because Hu-AGT was normally synthesized by hepatocytes (6), its synthesis was decreased in T-SV40–positive hepatocytes in a majority of nodules. This explains its decrease in synthesis and in plasma levels. Thus, the escape observed from this stage was related to the decrease in Hu-AGT synthesis and/or secretion.

We and others have shown that vascular endothelial growth factor (VEGF) up-regulates Dll4 in endothelial cells (20, 21) and Dll4 down-regulates VEGFR-2 and up-regulates VEGFR-1 (33). Because AGT reduced the number of proliferating hepatocytes, local VEGF concentrations might be impaired, leading to the reduction of Dll4 and active Notch4 observed in bitransgenic mice.

Adenovirus-mediated gene transfer of Hu-AGT into human mammary breast carcinoma (MDA-MB-231) inhibits tumor growth and tumor angiogenesis (13). Moreover, in mice overexpressing Hu-AGT, the number of murine B16F10 melanoma pulmonary metastasis was reduced compared with normal mice (13). Interestingly, circulating high serum levels of Hu-AGT strongly block the dissemination of B16F10 metastases, but did not inhibit the growth of pre-established subcutaneous MDA-MB-231 (13), thus suggesting that an antiangiogenic and antitumoral effect requires a high local concentration of Hu-AGT. Indeed, high local Hu-AGT expression has been shown to inhibit the growth of kidney artery walls in mice overexpressing AGT (34).

Our data show that AGT is a potent antiangiogenic factor *in vivo*. It is increasingly evident that multiple positive and negative

Published OnlineFirst March 24, 2009; DOI: 10.1158/0008-5472.CAN-08-2484

regulatory factors are involved in the control of tumor growth and angiogenesis in our model. At the latest stage, the liver architecture was progressively destroyed with a dramatic loss of hepatic functions leading to decreased synthesis of Hu-AGT (35). Moreover, because hepatocarcinoma is genetically committed to precocious death, the tumor growth evolution could be delayed early.

The antiangiogenic and antitumoral effects of AGT are most likely attributable to its serpin structure. Indeed, as shown by Célérier and colleagues, AGT can be modeled according to the structure of serpins (8). Recently, several serpins have been shown to have antiangiogenic activities (9–12). Maspin has been found to inhibit tumor progression and metastasis in mice (36). Furthermore, pigment epithelium-derived factor inhibits VEGF-induced angiogenesis by a cleavage and intracellular translocation of the transmembrane domain of VEGFR-1 (37). This regulated intramembrane proteolysis was dependent on γ-secretase. AGT might modulate positively or negatively intramembrane proteolysis such as Notch activation which is dependent on the γ-secretase complex.

Finally, we provide evidence that AGT exerts an *in vivo* antiangiogenic effect with a tendency to protect the tumor sinusoids from their arterial remodeling resulting in antitumor effects. AGT may represent an interesting strategy in the development of new antiangiogenic molecules.

Disclosure of Potential Conflicts of Interest

No potential conflicts of interest were disclosed.

Acknowledgments

Received 6/30/08; revised 1/22/09; accepted 1/22/09; published OnlineFirst 3/24/09.

Grant support: European Vascular Genomics Network, the Association Limousine Promotion Hospitalisation à Domicile and Association de Physiologie de la Faculté de Médecine de Limoges, France.

The costs of publication of this article were defrayed in part by the payment of page charges. This article must therefore be hereby marked *advertisement* in accordance with 18 U.S.C. Section 1734 solely to indicate this fact.

The authors thank Professor C.D. Sigmund from the Departments of Medicine and Physiology & Biophysics, University of Iowa College of Medicine, Iowa City, IA, United States, for the gift of the Hu-AGT-TG mice; Dr. M. Druet-Cabanac from Registre Général des Cancers en Région Limousin, Hôpital Universitaire de Limoges, France for his help in statistical analysis; Marie-Thérèse Morin and Anaïs Caillard for excellent technical assistance; and Herve Kempf for his help in manuscript editing.

References

1. Carmeliet P. Angiogenesis in health and disease. Nat Med 2003;9:653–60.
2. Ferrara N, Kerbel RS. Angiogenesis as a therapeutic target. Nature 2005;438:967–74.
3. Jain RK. Normalization of tumor vasculature: an emerging concept in antiangiogenic therapy. Science 2005;307:58–62.
4. Célérier J, Cruz A, Lamande N, Gasc JM, Corvol P. Angiotensinogen and its cleaved derivatives inhibit angiogenesis. Hypertension 2002;39:224–8.
5. Brand M, Lamande N, Larger E, Corvol P, Gasc JM. Angiotensinogen impairs angiogenesis in the chick chorioallantoic membrane. J Mol Med 2007;85:451–60.
6. Tewksbury D. Angiotensinogen: biochemistry and molecular biology. In: Laragh JH, Brenner GM, eds. Hypertension. New York: Raven Press; 1990. p. 1197–216.
7. Corvol P, Jeunemaitre X. Molecular genetics of human hypertension: role of angiotensinogen. Endocr Rev 1997; 18:662–77.
8. Celerier J, Schmid G, Le Caer JP, et al. Characterization of a human angiotensinogen cleaved in its reactive center loop by a proteolytic activity from Chinese hamster ovary cells. J Biol Chem 2000;275:10648–54.
9. O'Reilly MS, Pirie-Shepherd S, Lane WS, Folkman J. Antiangiogenic activity of the cleaved conformation of the serpin antithrombin. Science 1999;285:1926–8.
10. Zhang M, Volpert O, Shi YH, Bouck N. Maspin is an angiogenesis inhibitor. Nat Med 2000;6:196–9.
11. Dawson DW, Volpert OV, Gillis P, et al. Pigment epithelium-derived factor: a potent inhibitor of angiogenesis. Science 1999;285:245–8.
12. Miao RQ, Agata J, Chao L, Chao J. Kallistatin is a new inhibitor of angiogenesis and tumor growth. Blood 2002; 100:3245–52.
13. Bouquet C, Lamande N, Brand M, et al. Suppression of angiogenesis, tumor growth, and metastasis by adenovirus-mediated gene transfer of human angiotensinogen. Mol Ther 2006;14:175–82.
14. Yang G, Merrill DC, Thompson MW, Robillard JE, Sigmund CD. Functional expression of the human angiotensinogen gene in transgenic mice. J Biol Chem 1994;269:32497–502.
15. Dubois N, Bennoun M, Allemand I, et al. Time-course development of differentiated hepatocarcinoma and lung metastasis in transgenic mice. J Hepatol 1991;13: 227–39.
16. Dupuy E, Hainaud P, Villemain A, et al. Tumoral angiogenesis and tissue factor expression during hepatocellular carcinoma progression in a transgenic mouse model. J Hepatol 2003;38:793–802.
17. Lawson ND, Scheer N, Pham VN, et al. Notch signaling is required for arterial-venous differentiation during embryonic vascular development. Development 2001;128:3675–83.
18. Carlson TR, Yan Y, Wu X, et al. Endothelial expression of constitutively active Notch4 elicits reversible arteriovenous malformations in adult mice. Proc Natl Acad Sci U S A 2005;102:9884–9.
19. Gale NW, Baluk P, Pan L, et al. Ephrin-B2 selectively marks arterial vessels and neovascularization sites in the adult, with expression in both endothelial and smooth-muscle cells. Dev Biol 2001;230:151–60.
20. Patel NS, Li JL, Generali D, Poulsom R, Cranston DW, Harris AL. Up-regulation of Delta-like 4 ligand in human tumor vasculature and the role of basal expression in endothelial cell function. Cancer Res 2005;65:8690–7.
21. Hainaud P, Contreres JO, Villemain A, et al. The role of the vascular endothelial growth factor-Delta-like 4 ligand/Notch4-ephrin B2 cascade in tumor vessel remodeling and endothelial cell functions. Cancer Res 2006;66:8501–10.
22. Bonnin P, Villemain A, Vincent F, et al. Ultrasonic assessment of hepatic blood flow as a marker of mouse hepatocarcinoma. Ultrasound Med Biol 2007;33:561–70.
23. Sibony M, Commo F, Callard P, Gasc JM. Enhancement of mRNA *in situ* hybridization signal by microwave heating. Lab Invest 1995;73:586–91.
24. Clauser E, Bouhnik J, Jaramillo HN, Auzan C, Corvol P, Menard J. Angiotensinogen production and consumption in the adrenalectomized rat. Endocrinology 1985; 116:274–80.
25. Menard J, Catt KJ. Measurement of renin activity, concentration and substrate in rat plasma by radioimmunoassay of angiotensin I. Endocrinology 1972;90: 422–30.
26. Sugimoto H, Kaneko T, Hirota M, Inoue S, Takeda S, Nakao A. Physical hemodynamic interaction between portal venous and hepatic arterial blood flow in humans. Liver Int 2005;25:282–7.
27. Straub AC, Stolz DB, Ross MA, et al. Arsenic stimulates sinusoidal endothelial cell capillarization and vessel remodeling in mouse liver. Hepatology 2007;45:205–12.
28. Li JL, Sainson RC, Shi W, et al. Delta-like 4 Notch ligand regulates tumor angiogenesis, improves tumor vascular function, and promotes tumor growth *in vivo*. Cancer Res 2007;67:11244–53.
29. Ridgway J, Zhang G, Wu Y, et al. Inhibition of Dll4 signalling inhibits tumour growth by deregulating angiogenesis. Nature 2006;444:1083–7.
30. Noguera-Troise I, Daly C, Papadopoulos NJ, et al. Blockade of Dll4 inhibits tumour growth by promoting non-productive angiogenesis. Nature 2006;444:1032–7.
31. Gale NW, Yancopoulos GD. Growth factors acting via endothelial cell-specific receptor tyrosine kinases: VEGFs, angiopoietins, and ephrins in vascular development. Genes Dev 1999;13:1055–66.
32. Wang HU, Chen ZF, Anderson DJ. Molecular distinction and angiogenic interaction between embryonic arteries and veins revealed by ephrin-B2 and its receptor Eph-B4. Cell 1998;93:741–53.
33. Harrington LS, Sainson RC, Williams CK, et al. Regulation of multiple angiogenic pathways by Dll4 and Notch in human umbilical vein endothelial cells. Microvasc Res 2008;75:144–54.
34. Brand M, Lamande N, Sigmund CD, Larger E, Corvol P, Gasc JM. Angiotensinogen modulates renal vasculature growth. Hypertension 2006;47:1067–74.
35. Thorgeirsson SS, Grisham JW. Molecular pathogenesis of human hepatocellular carcinoma. Nat Genet 2002;31:339–46.
36. Zhang M, Shi Y, Magit D, Furth PA, Sager R. Reduced mammary tumor progression in WAP-TAg/WAP-maspin bitransgenic mice. Oncogene 2000;19:6053–8.
37. Cai J, Jiang WG, Grant MB, Boulton M. Pigment epithelium-derived factor inhibits angiogenesis via regulated intracellular proteolysis of vascular endothelial growth factor receptor 1. J Biol Chem 2006;281: 3604–13.

Cancer Research
The Journal of Cancer Research (1916–1930) | The American Journal of Cancer (1931–1940)

AACR American Association for Cancer Research

Angiotensinogen Delays Angiogenesis and Tumor Growth of Hepatocarcinoma in Transgenic Mice

François Vincent, Philippe Bonnin, Maud Clemessy, et al.

Cancer Res 2009;69:2853-2860. Published OnlineFirst March 24, 2009.